WNT5A Expression Increases during Melanoma Progression and Correlates with Outcome

Philip D. Da Forno,[1] J. Howard Pringle,[1] Peter Hutchinson,[3] Joy Osborn,[3] Qiang Huang,[1] Linda Potter,[1] Rachael A. Hancox,[1] Alan Fletcher,[2] and Gerald S. Saldanha[1]

Abstract

Purpose: Wnt ligands play a major role in development and are important in cancer. Expression microarray analysis correlates one member of this family, WNT5A, to a subclass of melanomas with increased motility and invasion. There are no large studies of clinical samples primarily addressing the importance of WNT5A in melanoma progression or outcome. Therefore, this study aimed to assess the protein expression of WNT5A during melanoma progression and its effect on outcome.

Experimental Design: Expression of WNT5A was determined in a series of 59 primary melanomas with matched metastases. To provide a benchmark of progression against which to assess WNT5A, expression of $p16^{ink4a}$ was analyzed, as this has been previously well documented in melanoma. The effect of WNT5A protein expression on outcome was assessed in 102 melanomas.

Results: Cytoplasmic WNT5A showed a trend of increasing expression with melanoma progression ($P = 0.013$), whereas there was diminishing $p16^{ink4a}$ expression ($P = 0.006$). Nevi showed relatively strong WNT5A expression. Strong cytoplasmic WNT5A was an independent risk factor for reduced metastasis-free and overall survival in multivariate analysis ($P = 0.001$ and 0.003, respectively).

Conclusion: Cytoplasmic WNT5A increases with melanoma progression and strong expression is associated with poor outcome.

Wnt proteins are a family of ligands whose functions are well known in embryonic development but are increasingly recognized as key proteins in cancer (1). One member of the family, WNT5A, has been found to play a role in several cancers (2–8). In particular, expression of WNT5A has been found to correlate with an aggressive phenotype in melanoma (4, 9, 10). At present, there are few studies of WNT5A using large sets of clinical melanoma tissue samples, making it difficult to accurately assess its value for predicting outcome or as a potential target for therapy. Such information is important because cutaneous melanoma (CM) is an increasingly common malignancy. Better understanding of metastatic disease is especially important because this can occur very early during progression and entails an extremely poor prognosis.

Authors' Affiliations: [1]Department of Cancer Studies and Molecular Medicine, University of Leicester; Departments of [2]Histopathology and [3]Dermatology, University Hospitals of Leicester NHS Trust, Leicester, United Kingdom

Received 12/7/07; revised 4/16/08; accepted 5/1/08.

Grant support: Pathological Society of Great Britain and Ireland.

The costs of publication of this article were defrayed in part by the payment of page charges. This article must therefore be hereby marked *advertisement* in accordance with 18 U.S.C. Section 1734 solely to indicate this fact.

Note: P.D. Da Forno, J.H. Pringle, and G.S. Saldanha contributed equally to this work.

Requests for reprints: Gerald Saldanha, Department of Cancer Studies and Molecular Medicine, University of Leicester, Level 3 RK-CSB, Leicester Royal Infirmary, Leicester LE2 7LX, United Kingdom. Phone: 44-116-252-3228; Fax: 44-116-254-1414; E-mail: gss4@le.ac.uk.

doi:10.1158/1078-0432.CCR-07-5104

WNT5A is a ligand in the noncanonical Wnt signaling pathway (10). On interacting with Frizzled, it activates a signal transduction cascade resulting in increased activity of protein kinase C and elevated intracellular Ca^{2+}. WNT5A has also been shown to inhibit β-catenin signaling, a key process in the canonical Wnt pathway (11). The role of WNT5A in CM progression is unclear but several studies suggest it may be important. Bittner et al. (9) found that low WNT5A expression could be used to define a group of CM with similar gene expression profiles and that, *in vitro*, this group had reduced cell motility and invasiveness. Conversely, high expression of WNT5A was found to lead to increased motility and invasion *in vitro* in melanoma cells, and in clinical samples, WNT5A protein expression increased during progression and showed a correlation with poor outcome (10). However, the data on clinical samples were preliminary as only small numbers were analyzed, paving the way for a detailed study of the role of WNT5A.

CM has several clinicopathologically recognizable premalignant and malignant phases, as described by Clark's model (12, 13). These are the following: the common acquired nevus, a usually stable benign lesion from which melanoma very occasionally arises; radial growth phase (RGP) melanoma, which has intraepidermal or minimally invasive growth and virtually no metastatic potential; vertical growth phase (VGP) melanoma, where the tumor has now progressed to frank invasion and has metastatic potential; and metastatic melanoma. Correlating molecular alterations to these recognizable patterns of tumor growth might allow key components of melanoma progression to be identified. This strategy has been

used in studies of $p16^{ink4a}$ expression loss, which were then linked to particular parts of Clark's progression model (14–17). The aims of this study were to evaluate the expression of WNT5A during CM progression and to use the comparatively well-characterized alterations in $p16^{ink4a}$ protein expression to serve as a benchmark for comparison. In addition, this study sought to show whether WNT5A expression correlated with CM metastasis-free and overall survival.

Materials and Methods

Tissues and cell lines. Fifty-nine cases of primary CM (mean Breslow depth, 4.34 mm; SD, 3.14 mm) with matched metastases were selected from the tissue archives of the University Hospitals of Leicester, with local research ethics committee approval. A search for melanoma metastases was done from 1988 to 2003. Sequential cases with sufficient material remaining in the tissue block were selected. The primary tumors were from the lower extremities in 21 cases (35.6%), the trunk in 18 cases (30.5%), the upper extremities in 8 cases (13.6%), the head and neck in 8 cases (13.6%), and acral in 3 cases (5.1%), and in one case site was unknown (1.7%). Of the 59 metastases, 45 were in lymph nodes (76.3%), 11 in skin (18.6%), 2 in s.c. tissue (3.4%), and 1 in the liver (1.7%). In addition, 20 nevi and 35 RGP melanomas were identified from sequential cases retrieved from the University Hospitals of Leicester pathology archives in 2004.

A further set of melanomas was used in survival analysis (see below). These were retrieved from a database of cases that had been under follow-up in the dermatology department, University Hospitals of Leicester. This was an unbiased cohort of patients collected from 1983. Fifty cases were selected in an entirely random manner. After exclusions (6, block too thin; 1, not melanoma), there were 43 cases. They had a mean Breslow thickness of 1.68 mm (SD, 1.49 mm). Of these, 3 were from the head and neck, 7 from the lower limb, 8 from the upper limb, and 18 from the trunk, and in 7 the site was not documented. These 43 cases were combined with the 59 primary melanomas with matched metastases described above, yielding 102 primary CMs for survival analysis. The overall mean Breslow thickness for the 102 cases was 3.16 mm (SD, 2.77). All tissues were formalin fixed and paraffin embedded.

Melanoma cell lines (SKMel2, SKMel5, and SKMel28) were obtained from the American Type Culture Collection, whereas A375P (parental low metastatic) and A375M1 (metastatic; ref. 18) were supplied by the European Collection of Animal Cell Cultures. All of the American Type Culture Collection cell lines were maintained in EMEM (Sigma) plus 2 mmol/L L-glutamine and 10% fetal bovine serum, whereas A375P and A375M1 were maintained in RPMI 1640 supplemented with 2 mmol/L L-glutamine and 10% fetal bovine serum. Cultures were split or used at subconfluent densities less than 70% to 80% and maintained for no longer than 4 wk after recovery from frozen stocks. Cytoblocks of each cell line were prepared from suspensions of cells (2×10^6/mL) fixed for 30 min at room temperature in 10% formol saline. The cytoblock technique was done with the Shandon kit according to the manufacturer's instructions (Shandon, Inc.) The button of cells formed was routinely processed and paraffin embedded.

Western blotting. The expression levels of WNT5A were determined by Western blotting of melanoma cell lines SKMel2, SKMel5, SKMel28, A375P, and A375M1. Cells were counted and 3×10^6 cells were lysed in ice-cold Gold Lysis Buffer containing a protease inhibitor cocktail (Sigma). The protein concentration of the lysates was quantified on a Lambda 25 UV/VIS spectrophotometer at 595 nm using the bovine serum albumin protein assay. Total protein (25 μg) was loaded onto 10% (w/v) SDS-polyacrylamide gels. PAGE was run at 100 V for ~1 h. The gel was washed once in transfer buffer (1.3 mmol/L SDS, 39 mmol/L glycine, 48 mmol/L Tris, 20% methanol) and electro-transferred onto a nitrocellulose membrane (Hybond ECL, Amersham Biosciences) using a wet transfer blot unit (Bio-Rad) at 100 V for 1 h at 4°C. Nonspecific binding sites were blocked by shaking the membrane at room temperature in TBS, 5% milk, and 1% Tween (TBST) for 1 h and then incubated overnight at 4°C with the primary polyclonal antibody goat anti-mouse WNT5A (0.2 μg/mL; diluted 1:500; R&D Systems). A secondary antibody, biotinylated rabbit anti-goat Ig (1:1,000; Dako), was added for 1 h followed by streptavidin-biotin complex horseradish peroxidase (Dako) following the manufacturer's instructions. Blots were detected using an enhanced chemiluminescence detection kit (Amersham Biosciences). Membranes were subsequently stripped by incubation in 15% (v/v) hydrogen peroxide in PBS for 1 h and washed thrice in TBST before reprobing with a loading control, mouse monoclonal anti-β-actin (diluted 1:2,000; Sigma), and incubated overnight at 4°C. A secondary antibody, sheep anti-mouse IgG peroxidase conjugated (diluted 1:2,000; GE Healthcare), was incubated for 1 h at room temperature before detection by enhanced chemiluminescence (Amersham Biosciences). The sizes of bands detected were compared with Precision Plus Protein standards (Bio-Rad).

mRNA analysis. Polyadenylated RNA was extracted from cell cultures using oligo(dT)-labeled paramagnetic beads according to the manufacturer's instructions (Dynal). A cell lysate was produced from a monolayer of cells by washing them in sterile cold PBS. Approximately 2×10^5 cells were resuspended in 250 μL of lysis binding buffer [100 mmol/L Tris-HCl (pH 8.0), 500 mmol/L LiCl, 10 mmol/L EDTA (pH 8.0), 1% (w/v) SDS, 5 mmol/L DTT] and passed through the pipette tip repeatedly to achieve complete lysis of the cells, which was stored at -20°C until RNA extraction with Dynabeads could be done.

Polyadenylated RNA was extracted and processed using oligo(dT)-linked Dynabeads (Dynal), as described previously (19). Briefly, cell lysate in lysis/binding buffer was incubated with 50 μg/mL proteinase K (Boehringer Mannheim) for 1 h at 37°C. The lysate was centrifuged for 30 s at 10,000 × *g*, and the supernatant was mixed with oligo(dT)-linked Dynabeads. The mRNA was allowed to anneal to the Dynabeads for 10 min at room temperature. RNA-linked Dynabeads were washed twice in a buffer containing LiDS [10 mmol/L Tris-HCl (pH 8), 0.15 mol/L LiCl, 1 mmol/L EDTA, 0.1% LiDS; Dynal] and thrice in the same buffer but without LiDS. Dynabeads were finally resuspended in diethyl pyrocarbonate water. Reverse transcription reactions were carried out at 42°C for 1 h using Expand reverse transcriptase (Boehringer Mannheim) in accordance with the manufacturer's instructions. In a total volume of 25 μL, reactions contained 5 μL Expand reverse transcriptase buffer, 10 mmol/L DTT, 1 mmol/L each of deoxynucleotide triphosphates (all from Boehringer Mannheim), and 30 units RNasin (Promega) in diethyl pyrocarbonate–treated water. To the positive reverse transcriptase reactions, 50 units of reverse transcriptase were added, and to the negative reverse transcriptase reactions, an equal volume of diethyl pyrocarbonate–treated water was added. Primers for WNT5A and glyceraldehyde-3-phosphate dehydrogenase (GAPDH; see Table 1) were used and PCR was done using a Perkin-Elmer thermocycler. Reactions were carried out with 1 to 2 μL of cDNA template in a total volume of 50 μL containing PCR buffer [45 mmol/L Tris (pH 8.8), 11 mmol/L $(NH_4)_2SO_4$, 4.5 mmol/L $MgCl_2$, 200 mmol/L deoxynucleotide triphosphates, 110 μg/mL bovine serum albumin, 6.7 mmol/L β-mercaptoethanol, 4.4 mmol/L EDTA (pH 8.8)] and 10 pmol each of forward and reverse primers. DNA was denatured

Table 1. Primers used for RT-PCR

Primer	Sequence	Gene position
GAPDH (forward)	AGAACATCATCCCTGCCTC	NM_002046 713-731
GAPDH (reverse)	GCCAAATTCGTTGTCATACC	NM_002046 1040-1059
WNT5A (forward)	GAAATGCGTGTTGGGTTGAA	NM_003392.3 3135-3154
WNT5A (reverse)	AGGCATGGGTTTCCATTCTG	NM_003392.3 3313-3332

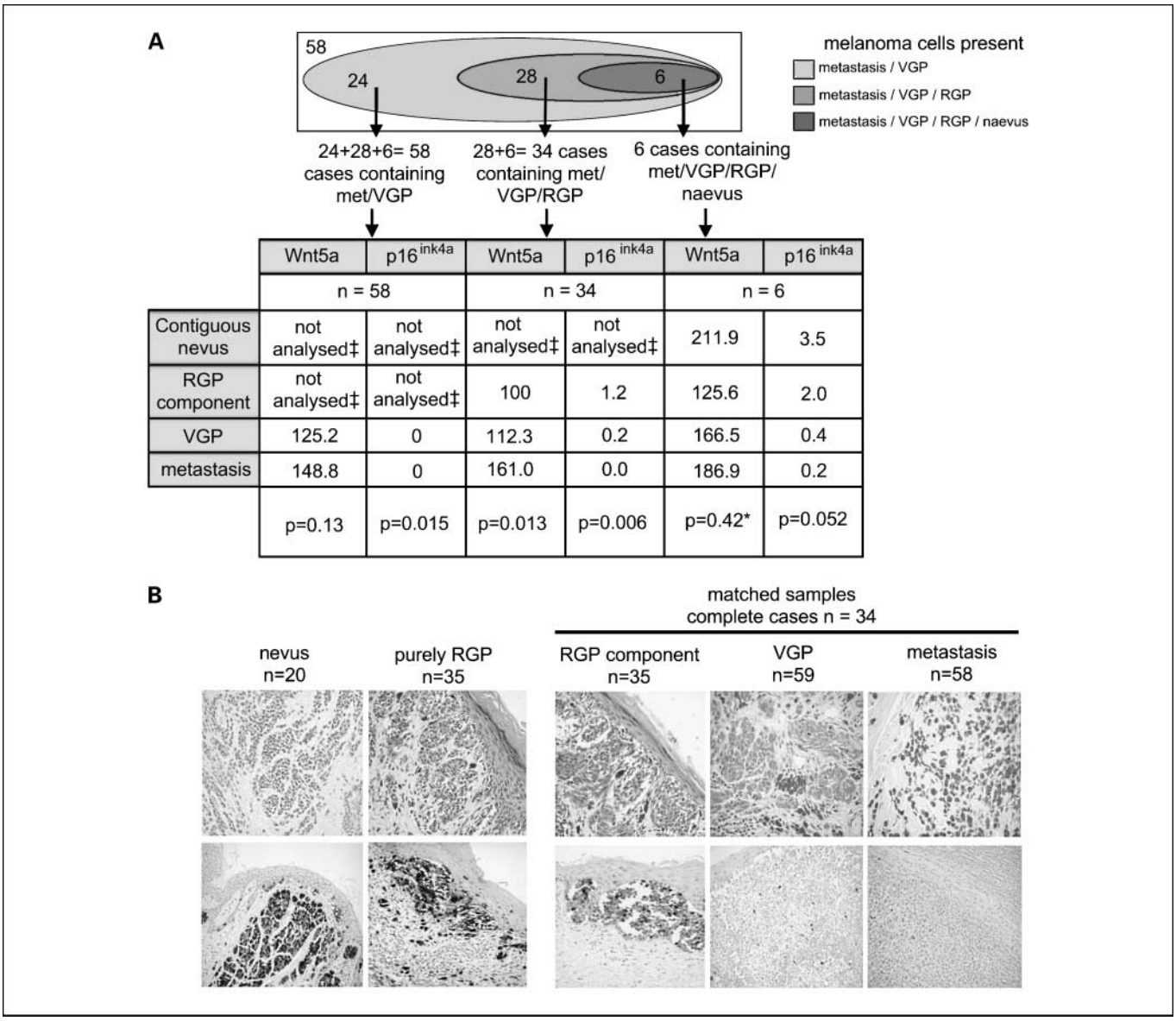

	Wnt5a	p16 ink4a	Wnt5a	p16 ink4a	Wnt5a	p16 ink4a
	n = 58		n = 34		n = 6	
Contiguous nevus	not analysed‡	not analysed‡	not analysed‡	not analysed‡	211.9	3.5
RGP component	not analysed‡	not analysed‡	100	1.2	125.6	2.0
VGP	125.2	0	112.3	0.2	166.5	0.4
metastasis	148.8	0	161.0	0.0	186.9	0.2
	p=0.13	p=0.015	p=0.013	p=0.006	p=0.42*	p=0.052

Fig. 1. Median cytoplasmic WNT5A immunoscores in matched primary and metastatic melanoma samples. *A,* subsets characterized by identified growth phases are shown in the Venn diagram. ‡, tumor components not analyzed because of absence in some cases. *B,* WNT5A and p16INK4a immunostaining.

at 94°C for 5 min and held at the primer annealing temperature during the addition of 1 IU of Taq polymerase (Promega) followed by an extension step at 72°C for 30 s. For all primers, the following cycle profile was used: 95°C for 30 s, 60°C for 30 s, 72°C for 30 s for 35 cycles, with a final extension step at 72°C for 7 min. The PCR products were loaded on a 2% Seakem agarose gel (BioWhittaker Molecular Applications) or 3% NuSieve agarose (Cambrex) containing 15 μg/mL ethidium bromide and gels were run at 150 V for 2 h. The resulting bands were visualized on a UV transilluminator and images were captured using a gel documentation system.

Immunohistochemistry. For $p16^{ink4a}$, antigen retrieval was achieved by microwaving sections immersed in 10 mmol/L citrate buffer for 20 min at 750 W. No antigen retrieval was used for the WNT5A antibody. Tissue sections (4 μm) were rehydrated and blocked in normal rabbit serum (Dako). Mouse WNT5A-specific goat IgG as used by Weeraratna et al. (1:40; R&D Systems; ref. 10) and mouse anti-human $p16^{ink4a}$ (1:30; BD PharMingen) were applied and incubated at 4°C. Detection was via biotinylated rabbit anti-goat Ig (1:600; Dako) for WNT5A and rabbit anti-mouse (Dako) for $p16^{ink4a}$ followed by streptavidin-biotin complex alkaline phosphatase (Dako). WNT5A was visualized in naphthol AS-BI phosphate and Fast Red TR in the presence of levamisole. $p16^{ink4a}$ was visualized by 10-min incubation with nitroblue tetrazolium chloride/5-bromo-4-chloro-3-indolyl phosphate, toluidine salt (Roche Diagnostics). The $p16^{ink4a}$ antibody had been used in previously published studies (20–22). Assays were run parallel with positive (breast myoepithelium for WNT5A; common acquired nevus for $p16^{ink4a}$) and negative (primary antibody omitted) controls. Cytoplasmic and nuclear WNT5A was scored via a semiquantitative method based on the H-SCORE (23). This provided a score between 0 and 300. Two observers agreed on reference fields graded as weak, moderate, and intense staining. These were photographed and used as a guide for scoring all cases. Interobserver agreement was measured using 12 randomly selected cases and an intraclass correlation coefficient indicated high agreement {intraclass correlation coefficient of 0.94 [95% confidence interval (95% CI), 0.82-0.98] for cytoplasmic staining and 0.91 (95% CI, 0.84-0.98) for nuclear staining}. A single observer

then scored WNT5A staining. Three observers agreed the criteria for positive $p16^{ink4a}$ nuclear staining and all sections were subsequently scored. Five hundred cells chosen from randomly sampled areas of the tumor or tumor growth phase in question were scored as having either positive or negative nuclear staining. From this, a percentage of $p16^{ink4a}$-positive cells within the tumor or tumor phase was derived.

Statistical analysis. Nonparametric analyses were done. These included Mann-Whitney test for unmatched pairs and Page's *L* test for trend analysis of related samples. Analyses were done using Statistical Package for the Social Sciences release 12.0, except Page's *L* test, which was calculated manually. Survival was analyzed for two outcomes: time to metastasis and time to death from any cause. Times were calculated in months from the date of primary melanoma diagnosis to the date of event. For metastasis, patients were censored at last follow-up or time of death if it was unrelated to melanoma. For time to death, patients remaining alive were censored at last follow-up. Survival curves were generated according to the Kaplan-Meier product-limit method and were compared using the log-rank test for trend. Univariate and multivariate analyses of prognostic factors were based on the Cox proportional hazards model. The prognostic factors included in the multivariate analysis of primary melanoma were the following: age at diagnosis (≤60 y or >60 y), sex, primary melanoma site (extremities versus trunk, head and neck, or acral sites), Breslow thickness (coded as ≤2.00 mm, between 2.01 and 4 mm, and >4 mm), nuclear WNT5A (cut into score tertiles), and cytoplasmic WNT5A (cut into score tertiles). The coding for clinical covariates was based on previously used definitions (24). All variables were entered into the final regression model without variable selection procedures. The covariates obeyed the assumption of proportionality and there was no evidence of multicollinearity.

Results

WNT5A expression during tumor progression. Preliminary data, based on a single case, suggested that WNT5A protein expression increased with progression (10). To extend this finding, a set of 59 primary melanomas with matched metastases was analyzed. In addition, we analyzed $p16^{ink4a}$ (14, 15, 17, 25–28) to provide a benchmark against which to assess WNT5A expression.

From 58 primary VGP melanomas and their matched metastases (one of the original 59 matched pairs was excluded because the metastasis was necrotic), subgroups were identified based on whether cells from different phases of progression were present. The way these subgroups were extracted from the starting group of 58 melanomas and their matched metastases is illustrated in Fig. 1A alongside the median immunostaining scores for cytoplasmic WNT5A and nuclear $p16^{ink4a}$. Photomicrographs of immunostaining are shown in Fig. 1B, these being reference fields used for scoring cytoplasmic WNT5A (see methods above). Malignant parts of the tumors (i.e., RGP, VGP, and metastasis) showed a significant trend of increasing cytoplasmic WNT5A expression with progression ($P = 0.013$). Contiguous nevus cells were present in six cases and showed median cytoplasmic WNT5A staining that was higher than any part of the matched melanoma, explaining why no trend was seen in these cases ($P = 0.42$). A mosaic pattern of nuclear $p16^{ink4a}$ staining was seen, as described by others (29, 30). A trend of decreasing $p16^{ink4a}$ was seen during progression in the 34 cases containing RGP, VGP, and metastasis ($P = 0.006$) and fell just short of significance in the 6 nevus-containing cases ($P = 0.052$).

High WNT5A expression in nevi. The finding of high WNT5A protein expression in nevi has not been described previously and differs from previous findings (2, 10). However, the six melanoma-associated nevi were a small sample and were biased toward those that had progressed to CM, thus were unrepresentative of nevi in general. Therefore, to validate this finding, an independent set of 20 common nevi (i.e., without associated melanoma) and 35 purely RGP melanomas (i.e., with no VGP) was analyzed (see Fig. 2). The cytoplasmic WNT5A staining score was significantly higher in these nevi than that in the 35 purely RGP melanomas (median, 144.3 and 69.2, respectively; $P = 0.04$), suggesting that WNT5A expression is genuinely high in nevi. To ensure that the findings were not related to a specific batch of antibody, 8 of the 20 common nevi with sufficient tissue were selected, including examples with both relatively strong and weak WNT5A. These were restained with a new batch of antibody. Replicate staining of a nevus with two batches of antibody is shown in Fig. 3A. An intraclass correlation coefficient was calculated to determine the level of agreement between these eight cases. A value of 0.82 indicated almost perfect agreement (31, 32). As a last validation step, we looked for evidence that the WNT5A antibody was detecting the appropriate protein in formalin-fixed, paraffin-embedded material, this being the starting material for our nevus and melanoma samples. To do this, formalin-fixed, paraffin-embedded cytoblocks were prepared from melanoma cell lines, some of which had known expression. Immunostaining for WNT5A in these samples was then compared with expression in fresh samples of matched cells, as measured by reverse

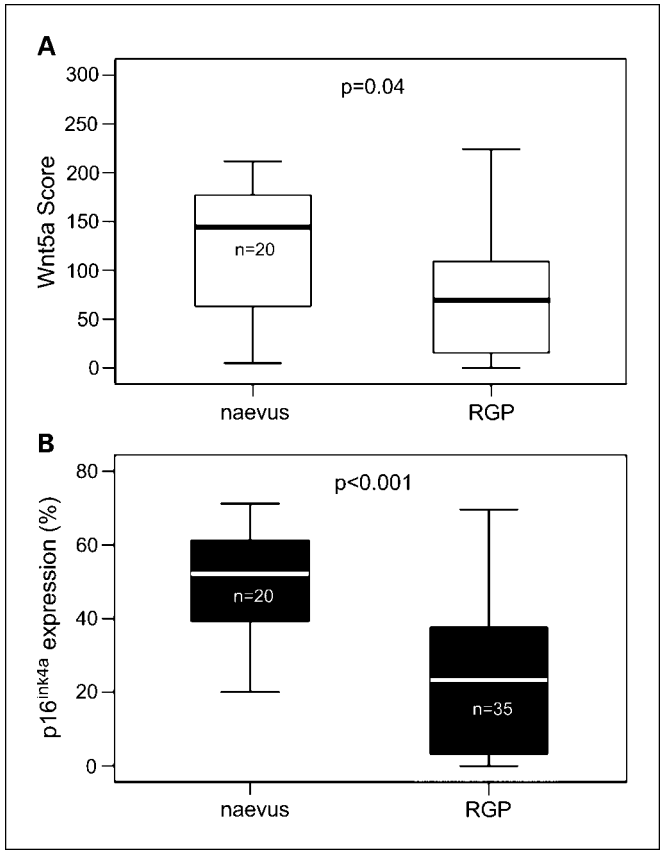

Fig. 2. WNT5A and $p16^{INK4a}$ immunostaining in common acquired nevi and purely RGP tumors. The box plots show differences in expression of WNT5A (*A*) and $p16^{ink4a}$ (*B*) between isolated common acquired nevi and purely RGP melanoma. The significance of these differences is shown.

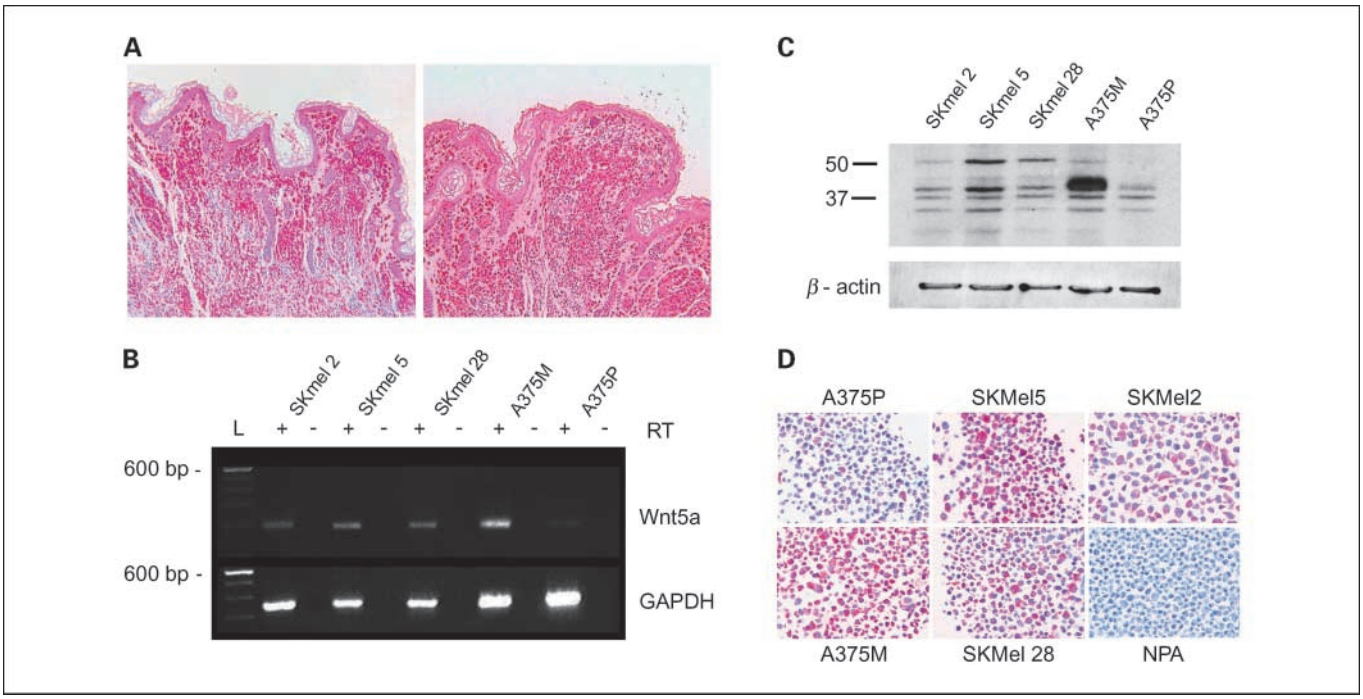

Fig. 3. Strong WNT5Aexpression in nevi. *A,* single nevus stained with two different batches of the WNT5A antibody. Strong staining was seen in both sections. *B,* WNT5A RT-PCR. *C,* WNT5A Western blotting. The 42-kDa band represents unprocessed WNT5A precursor; the bands in the range 38 to 42 kDa and at ~22 kDa have also been reported as WNT5A molecules; the 50-kDa band corresponds to secreted protein. *D,* immunohistochemistry of formalin-fixed, paraffin-embedded cell line cytoblocks. Overall, the degree of WNT5A staining in the cytoblocks is commensurate with RT-PCR and Western blotting for each cell line. NPA, no primary antibody.

transcription-PCR (RT-PCR) and Western blot. The results are shown in Fig. 3B to D. This showed that cytoblock expression detected by immunocytochemistry was commensurate with levels of expression measured by RT-PCR and Western blotting in fresh material. The bands observed by Western blotting showed similar sizes to those reported by Peters et al. (33), who used the same antibody and confirmed the specificity of the bands by immunoprecipitation and preabsorption of the anti-WNT5A antibody by an immunizing peptide. The 50-kDa, 42-kDa, 38- to 42-kDa, and 22-kDa bands have all been reported as WNT5A molecules, the 50-kDa band being the secreted molecule (33, 34). Furthermore, A375P and A375M1 have been directly compared for WNT5A mRNA expression previously using microarray analysis [see Supplementary Table in Clark et al. (35)], with A375M1 being a metastasizing strain of the weakly metastasizing parental line, A375P. Our results agree with those findings, with A375M1 showing much higher expression of WNT5A. The $p16^{ink4a}$ score in the 20 isolated nevi was significantly higher than that in the 35 purely RGP melanomas (median, 52.1 and 29.1, respectively; $P < 0.001$).

WNT5A expression and outcome. The 59 primary melanomas with matched metastases were combined with a further 43 primary melanomas from a database of consecutive cases with known outcome, yielding a total of 102 cases. The 35 purely RGP melanomas were not included because such melanomas are not believed to have metastatic potential (12). Nuclear WNT5A was also assessed, as this has been previously analyzed by Bachmann et al. (2).

Survival was initially assessed using Kaplan-Meier analysis by arbitrarily dividing the cases into tertiles of WNT5A immunoscores. The results are shown in Fig. 4 with *P* values calculated using the log-rank test. An established prognostic marker, Breslow depth (36), is also shown. The findings for Breslow depth are in line with published results and thus lend some support for the validity of the WNT5A data. This preliminary analysis showed that the lower and middle tertile groups of cytoplasmic WNT5A immunostaining had similar survival and were therefore combined into a single group that was compared with the highest tertile for all regression analyses (similarly for nuclear WNT5A). Univariate and multivariate models were constructed using Cox proportional hazards regression. Eight cases with missing "site" data were omitted. The results are summarized in Table 2. In the univariate analysis, cytoplasmic WNT5A, Breslow thickness, and age were significant predictors of both time to metastasis and time to death from any cause. Male gender was a significant predictor of time to metastasis only. Site and nuclear WNT5A were not significant for either outcome. A multivariate model was developed and cytoplasmic WNT5A, Breslow thickness, gender, and age were all significant predictors of both time to metastasis and time to death from any cause. There was no evidence of a significant interaction between cytoplasmic WNT5A and Breslow thickness, suggesting that strong cytoplasmic WNT5A increases the hazard of metastasis regardless of melanoma depth. Together, these data suggest that cytoplasmic WNT5A is a risk factor for outcome in CM when controlling for other clinicopathologic variables.

Discussion

WNT5A expression during CM progression. Bittner et al. (9) concluded that CM cell lines expressing higher levels of WNT5A were more invasive and motile (9). This is in accord with the findings of the present study, where high levels of expression

were found in metastatic CM, in which motility is a requirement for cells to reach distant sites. Weeraratna et al. (10) described a single case of acral melanoma where intratumoral progression correlated with increased expression of WNT5A. We have greatly expanded on this preliminary data by showing, in 58 cases of matched primary and metastatic CM, that expression of WNT5A increases during progression. It should be noted that Weeraratna et al. studied membranous WNT5A, but their photomicrographs clearly show cytoplasmic staining.

The finding of high WNT5A protein expression in nevi is novel. In support of our findings, Pham et al. (37) identified high WNT5A mRNA in nevi. A recent microarray study using Affymetrix GeneChip Human Genome U133 Array Set HG-U133A to carry out expression profiles of primary malignant melanoma compared with benign skin nevi by Talantov et al. (38) also supports our results as they have shown that WNT5A mRNA is strongly expressed in the majority of nevi tested. However, Bachmann et al. (2) found higher nuclear expression but lower cytoplasmic WNT5A expression in nevi compared with a set of nodular melanomas. Weeraratna et al. (10) also found low expression in nevi. Although the present study and those of Weeraratna et al. and Bachmann et al. all used the same antibody, some of these discrepancies could be due to different methods of antigen retrieval, staining, and scoring, which were not identical between the studies. Because of these discrepancies, primarily relating to the level of WNT5A in nevi, we attempted to validate our findings. First, we ensured that the data were not due to variation between antibody batches, and second, we determined that the levels of WNT5A detected by the antibody in formalin-fixed, paraffin-embedded material were commensurate with levels detected by RT-PCR and Western blotting in fresh material. There was agreement between levels of expression by all methods at mRNA and protein levels, including formalin-fixed, paraffin-embedded samples. For A375P and A375M1, there was also independent corroboration from published data (35). The results supported the validity of the WNT5A antibody and support our findings.

Alterations of $p16^{ink4a}$ are comparatively well studied and were used as a benchmark against which cytoplasmic WNT5A expression could be examined. The finding that $p16^{ink4a}$ shows diminishing expression from nevus to metastasis is in accord with previous reports (14, 15, 26–28). Overall, these data indicate that CM shows progressive loss of $p16^{ink4a}$, whereas cytoplasmic WNT5A shows progressive increase.

The data allow some speculation as to possible interplay between the two alterations. It has been shown that induction of $p16^{ink4a}$ leads to premature senescence (30). It is likely therefore that loss of $p16^{ink4a}$ function in melanoma removes a melanocyte senescence barrier and allows uncontrolled proliferation. In this scenario, increasing WNT5A expression could allow further progression by affecting the additional cancer phenotypes of motility and invasion. A recent study sheds light on the mechanisms underpinning this effect (4): WNT5A, acting through protein kinase C, mediates epithelial-mesenchymal transition via Snail up-regulation and suppression of E-cadherin.

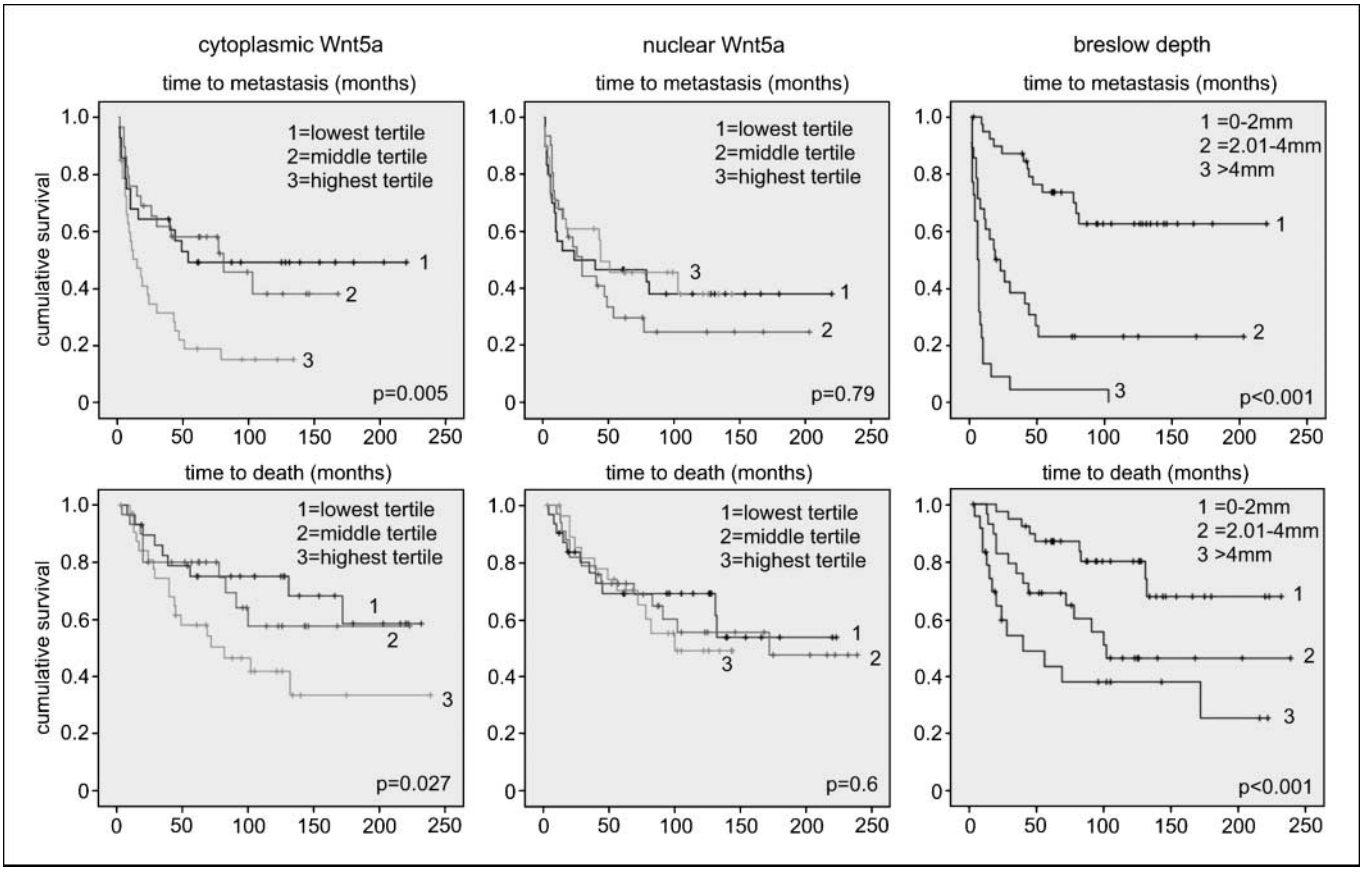

Fig. 4. Kaplan-Meier survival plots. The *P* value of a log-rank test for trend is shown for each plot.

Table 2. Regression analysis of survival

Outcome metastasis*		*n*	Univariate model		Multivariate model	
			HR (95% CI)	*P*	HR (95% CI)	*P*
Cytoplasmic WNT5A	Lowest tertiles	57	1		1	
	Upper tertile	33	2.5 (1.3-4.9)	0.007	3.3 (1.6-6.8)	0.001
Nuclear WNT5A	Lowest tertiles	61	1		1	
	Upper tertile	29	1.1 (0.5-2.1)	0.896	1.3 (0.6-2.9)	0.470
Breslow	0-2 mm	40	1		1	
	2.01-4 mm	28	3.8 (1.6-8.9)	0.002	3.6 (1.4-9.1)	0.006
	>4 mm	22	10.4 (4.2-26.1)	<0.001	7.4 (2.7-20.2)	<0.001
Site	Peripheral	42	1		1	
	Axial	48	0.9 (0.5-1.8)	0.797	0.5 (0.2-1.2)	0.113
Gender	Female	46	1		1	
	Male	44	2 (1.0-3.9)	0.042	3.2 (1.4-7.1)	0.005
Age	≤60	56	1		1	
	>60	34	3.5 (1.8-6.8)	<0.001	2.7 (1.3-5.4)	0.008
Outcome death*		***n***	**Univariate model**		**Multivariate model**	
			HR (95% CI)	***P***	**HR (95% CI)**	***P***
Cytoplasmic WNT5A	Lowest tertiles	59	1		1	
	Upper tertile	34	2.3 (1.2-4.5)	0.011	2.9 (1.4-5.9)	0.003
Nuclear WNT5A	Lowest tertiles	64	1		1	
	Upper tertile	29	1.0 (0.5-2.0)	0.985	1.2 (0.6-2.6)	0.637
Breslow	0-2 mm	40	1		1	
	2.01-4 mm	29	3.8 (1.6-8.8)	0.02	3.4 (1.4-8.5)	0.008
	>4 mm	24	10.9 (4.4-27.0)	<0.001	7.5 (2.8-20.1)	<0.001
Site	Peripheral	44	1		1	
	Axial	49	0.97 (0.5-1.9)	0.923	0.6 (0.3-1.3)	0.224
Gender	Female	49	1		1	
	Male	44	1.9 (1.0-3.6)	0.064	2.6 (1.2-5.8)	0.016
Age	≤60	57	1		1	
	>60	36	3.6 (1.9-7.0)	<0.001	2.6 (1.3-5.3)	0.007

*Cases where time to event was zero were excluded (four where metastasis was the outcome and one when death from any cause was the outcome). Eight of the original 102 cases were excluded because melanoma site of origin could not be established.

Epithelial-mesenchymal transition is believed to be a key event for acquisition of an invasive phenotype. Some speculation about high cytoplasmic WNT5A in nevi can also be made. It may induce a motile phenotype, similar to that in metastatic cells, thus allowing nevus cells to undergo their characteristic migration into the dermis. However, subsequent $p16^{ink4a}$ expression then induces senescence to prevent further progression. Alternatively, it is possible that WNT5A has different effects in nevi compared with melanoma because the different cell contexts result in activation of different downstream pathways. Thus, in the context of nevus cells, WNT5A activity might cause inhibition of canonical Wnt signaling, resulting in a tumor suppressor effect by restraining the oncogenic effects of nuclear β-catenin (11, 39). The subsequent marked reduction in WNT5A in cells that progress to the RGP might represent loss of this tumor-suppressive effect in early melanoma, whereas in advanced melanoma, as the cellular context changes yet again, the oncogenic effects of WNT5A signaling through protein kinase C might supervene (4, 10). Context-dependent changes such as these are akin to those described for the transcription factor MITF (40).

WNT5A and outcome. The samples in this study were biased toward thick metastatic lesions. Nevertheless, the analysis was helpful in providing a preliminary assessment of the contribution of cytoplasmic WNT5A expression to outcome, but the relevance to melanoma in general will require investigation of an unbiased sample of CMs. Previous studies of WNT5A expression and survival have been done. Weeraratna et al. (10) did a small study of tumor tissue, including 8 nevi, 10 primary melanomas, and 9 metastases, studying membranous WNT5A (although showing cytoplasmic staining, as mentioned above). These authors stated that WNT5A expression correlated strongly with both survival and time to metastasis. However, there was no statistical analysis to support this statement, with only four deaths recorded in total, and no correction for baseline variables such as Breslow depth. However, these authors do point out that their data from analysis of tumor tissues are preliminary and that further work on larger tumor series would be required. The data of the present study therefore extend that of Weeraratna et al. Bachmann et al. did a study that included both cytoplasmic and nuclear WNT5A staining. Nuclear WNT5A was tested as a predictor of 5- and 10-year survival rate and, as in our study, was not significant. The effect of cytoplasmic WNT5A on outcome was not explicitly stated. Given that WNT5A is a secreted ligand produced in both nevus and melanoma cells (37), its presence in the cytoplasm of these cells would be a reasonable marker of protein expression. However, the significance of its presence in the nucleus is unclear. In particular, it is difficult to be sure that this does not represent an artifact. There are no other reports of WNT5A in the nucleus, although it is known that other secreted ligands can be found in the nucleus, as with fibroblast growth factor 2

(41). Whatever the role of nuclear WNT5A, if indeed any, our results suggest that it is not important in prediction of survival in melanoma patients.

Conclusions. In summary, these data show that expression of cytoplasmic WNT5A increases with CM progression and that its expression is a risk factor for outcome. Further studies will be necessary to determine the extent to which the present findings are applicable to an unbiased sample of melanomas.

Disclosure of Potential Conflicts of Interest

No potential conflicts of interest were disclosed.

References

1. Polakis P. The many ways of Wnt in cancer. Curr Opin Genet Dev 2007;17:45–51.
2. Bachmann I, Straume O, Puntervoll H, Kalvenes M, Akslen L. Importance of P-cadherin, β-catenin and Wnt5a/frizzled for progression of melanocytic tumours and prognosis in cutaneous melanoma. Clin Cancer Res 2005;11:8606–14.
3. Bui TD, Tortora G, Ciardiello F, Harris AL. Expression of Wnt5a is downregulated by extracellular matrix and mutated c-Ha-ras in the human mammary epithelial cell line MCF-10A. Biochem Biophys Res Commun 1997;239:911–7.
4. Dissanayake SK, Wade M, Johnson CE, et al. The Wnt5A/protein kinase C pathway mediates motility in melanoma cells via the inhibition of metastasis suppressors and initiation of an epithelial to mesenchymal transition. J Biol Chem 2007;282:17259–71.
5. Medrano EE. Wnt5a and PKC, a deadly partnership involved in melanoma invasion. Pigment Cell Res 2007;20:258–9.
6. Khan NI, Bradstock KF, Bendall LJ. Activation of Wnt/β-catenin pathway mediates growth and survival in B-cell progenitor acute lymphoblastic leukaemia. Br J Haematol 2007;138:338–48.
7. Wang Q, Williamson M, Bott S, et al. Hypomethylation of WNT5A, CRIP1 and S100P in prostate cancer. Oncogene 2007;26:6560–5.
8. Huang CL, Liu D, Nakano J, et al. Wnt5a expression is associated with the tumor proliferation and the stromal vascular endothelial growth factor—an expression in non-small-cell lung cancer. J Clin Oncol 2005; 23:8765–73.
9. Bittner M, Meltzer P, Chen Y, et al. Molecular classification of cutaneous malignant melanoma by gene expression profiling. Nature 2000;406:536–40.
10. Weeraratna AT, Jiang Y, Hostetter G, et al. Wnt5a signaling directly affects cell motility and invasion of metastatic melanoma. Cancer Cell 2002;1:279–88.
11. Topol L, Jiang X, Choi H, Garrett-Beal L, Carolan PJ, Yang Y. Wnt-5a inhibits the canonical Wnt pathway by promoting GSK-3-independent β-catenin degradation. J Cell Biol 2003;162:899–908.
12. Clark WH, Jr., Elder DE, Guerry D IV, et al. Model predicting survival in stage I melanoma based on tumor progression. J Natl Cancer Inst 1989;81: 1893–904.
13. Miller AJ, Mihm MC, Jr. Melanoma. N Engl J Med 2006;355:51–65.
14. Keller-Melchior R, Schmidt R, Piepkorn M. Expression of the tumor suppressor gene product p16INK4 in benign and malignant melanocytic lesions. J Invest Dermatol 1998;110:932–8.
15. Reed JA, Loganzo F, Jr., Shea CR, et al. Loss of expression of the p16/cyclin-dependent kinase inhibitor 2 tumor suppressor gene in melanocytic lesions correlates with invasive stage of tumor progression. Cancer Res 1995;55:2713–8.
16. Sparrow LE, Eldon MJ, English DR, Heenan PJ. p16 and p21WAF1 protein expression in melanocytic tumors by immunohistochemistry. Am J Dermatopathol 1998;20:255–61.
17. Grover R, Chana JS, Wilson GD, Richman PI, Sanders R. An analysis of p16 protein expression in sporadic malignant melanoma. Melanoma Res 1998; 8:267–72.
18. Kozlowski JM, Hart IR, Fidler IJ, Hanna N. A human melanoma line heterogeneous with respect to metastatic capacity in athymic nude mice. J Natl Cancer Inst 1984;72:913–7.
19. Bicknell GR, Shaw JA, Pringle JH, Furness PN. Amplification of specific mRNA from a single human renal glomerulus, with an approach to the separation of epithelial cell mRNA. J Pathol 1996;180:188–93.
20. Serrano M, Hannon GJ, Beach D. A new regulatory motif in cell-cycle control causing specific inhibition of cyclin D/CDK4. Nature 1993;366:704–7.
21. Yeager T, Stadler W, Belair C, Puthenveettil J, Olopade O, Reznikoff C. Increased p16 levels correlate with pRb alterations in human urothelial cells. Cancer Res 1995;55:493–7.
22. Kamb A, Shattuck-Eidens D, Eeles R, et al. Analysis of the p16 gene (CDKN2) as a candidate for the chromosome 9p melanoma susceptibility locus. Nat Genet 1994;8:23–6.
23. Kinsel LB, Szabo E, Greene GL, Konrath J, Leight GS, McCarty KS, Jr. Immunocytochemical analysis of estrogen receptors as a predictor of prognosis in breast cancer patients: comparison with quantitative biochemical methods. Cancer Res 1989;49:1052–6.
24. Gimotty PA, Guerry D, Ming ME, et al. Thin primary cutaneous malignant melanoma: a prognostic tree for 10-year metastasis is more accurate than American Joint Committee on Cancer staging. J Clin Oncol 2004;22:3668–76.
25. Ghiorzo P, Villaggio B, Sementa AR, et al. Expression and localization of mutant p16 proteins in melanocytic lesions from familial melanoma patients. Hum Pathol 2004;35:25–33.
26. Talve L, Sauroja I, Collan Y, Punnonen K, Ekfors T. Loss of expression of the p16INK4/CDKN2 gene in cutaneous malignant melanoma correlates with tumor cell proliferation and invasive stage. Int J Cancer 1997; 74:255–9.
27. Straume O, Sviland L, Akslen LA. Loss of nuclear p16 protein expression correlates with increased tumor cell proliferation (Ki-67) and poor prognosis in patients with vertical growth phase melanoma. Clin Cancer Res 2000;6:1845–53.
28. Alonso SR, Ortiz P, Pollan M, et al. Progression in cutaneous malignant melanoma is associated with distinct expression profiles: a tissue microarray-based study. Am J Pathol 2004;164:193–203.
29. Gray-Schopfer V, Cheong S, Chong H, et al. Cellular senescence in naevi and immortalisation in melanoma: a role for p16? Br J Cancer 2006;95:496–505.
30. Michaloglou C, Vredeveld LC, Soengas MS, et al. BRAFE600-associated senescence-like cell cycle arrest of human naevi. Nature 2005;436:720–4.
31. Landis JR, Koch GG. An application of hierarchical κ-type statistics in the assessment of majority agreement among multiple observers. Biometrics 1977;33: 363–74.
32. Landis JR, Koch GG. The measurement of observer agreement for categorical data. Biometrics 1977;33: 159–74.
33. Peters S, Mix E, Bauer P, et al. Wnt-5a expression in the rat neuronal progenitor cell line ST14A. Exp Brain Res 2004;158:189–95.
34. Gavin BJ, McMahon JA, McMahon AP. Expression of multiple novel Wnt-1/int-1-related genes during fetal and adult mouse development. Genes Dev 1990;4: 2319–32.
35. Clark EA, Golub TR, Lander ES, Hynes RO. Genomic analysis of metastasis reveals an essential role for RhoC. Nature 2000;406:532–5.
36. Balch CM, Buzaid AC, Soong SJ, et al. Final version of the American Joint Committee on Cancer staging system for cutaneous melanoma. J Clin Oncol 2001; 19:3635–48.
37. Pham K, Milovanovic T, Barr RJ, Truong T, Holcombe RF. Wnt ligand expression in malignant melanoma: pilot study indicating correlation with histopathological features. Mol Pathol 2003;56:280–5.
38. Talantov D, Mazumder A, Yu JX, et al. Novel genes associated with malignant melanoma but not benign melanocytic lesions. Clin Cancer Res 2005; 11:7234–42.
39. Westfall TA, Brimeyer R, Twedt J, et al. Wnt-5/pipetail functions in vertebrate axis formation as a negative regulator of Wnt/β-catenin activity. J Cell Biol 2003; 162:889–98.
40. Garraway LA, Widlund HR, Rubin MA, et al. Integrative genomic analyses identify MITF as a lineage survival oncogene amplified in malignant melanoma. Nature 2005;436:117–22.
41. Sheng Z, Lewis JA, Chirico WJ. Nuclear and nucleolar localization of 18-kDa fibroblast growth factor-2 is controlled by C-terminal signals. J Biol Chem 2004;279:40153–60.